We are IntechOpen, the world's leading publisher of Open Access books Built by scientists, for scientists

4,800
Open access books available

122,000
International authors and editors

135M
Downloads

Our authors are among the

154
Countries delivered to

TOP 1%
most cited scientists

12.2%
Contributors from top 500 universities

CLARIVATE ANALYTICS BOOK CITATION INDEX INDEXED

WEB OF SCIENCE™

Selection of our books indexed in the Book Citation Index in Web of Science™ Core Collection (BKCI)

Interested in publishing with us?
Contact book.department@intechopen.com

Numbers displayed above are based on latest data collected.
For more information visit www.intechopen.com

Chapter 7

Non-Destructive Examination of Interfacial Debonding in Dental Composite Restorations Using Acoustic Emission

Haiyan Li, Jianying Li, Xiaozhou Liu and Alex Fok

Additional information is available at the end of the chapter

http://dx.doi.org/10.5772/51369

1. Introduction

Light-cured, dental resin composites are widely used to repair decayed or damaged teeth because of their superior esthetics, ease of use and ability to bond to tooth tissues. However, during setting or polymerization, the resin composite shrinks, producing shrinkage stresses within the tooth and composite [1]. If the internal shrinkage stress is high enough, debonding between the tooth and restoration will occur, causing problems such as reduced fracture resistance and increased micro-leakage. The latter will ultimately lead to secondary caries. Clinical studies have identified the loss of interfacial integrity as one of the main causes for replacement of composite restorations [2-4].

Unfortunately, interfacial debonding caused by the shrinkage of composite resins can be hard to avoid. Fig. 1 shows evidence of interfacial debonding by comparing the Micro-CT images of a restored tooth before and after curing the composite. It can be seen that an interfacial crack of a significant length appeared after curing the composite along the initially intact interface. On the other hand, in the example shown in Fig. 2, where a different resin composite was used, no clear interfacial debonding was observed from the Micro-CT images. Therefore, whether interfacial debonding will occur depends on the restorative composite material, specifically the level of shrinkage stress it produces. There are other factors that may affect the initial quality and subsequent degradation of bonding at the tooth-restoration interface, e.g. the adhesive/bonding materials, cavity geometry, restorative techniques, thermal and mechanical loading, etc. [5-8].

It is very difficult to predict whether interfacial debonding will take place in a particular composite restoration system. This is because the shrinkage stress within a real tooth restoration is difficult to predict or measure due to the small but complicated geometry and

rapidly changing material properties during curing. At the same time, the bond strength between the tooth and restoration is difficult to determine. Tensile and shear tests have been widely used for bond strength testing. However, the results are highly variable, being dependent on the test devices and specimen size used [9-11]. Therefore, they are not very predictive of the actual clinical performance.

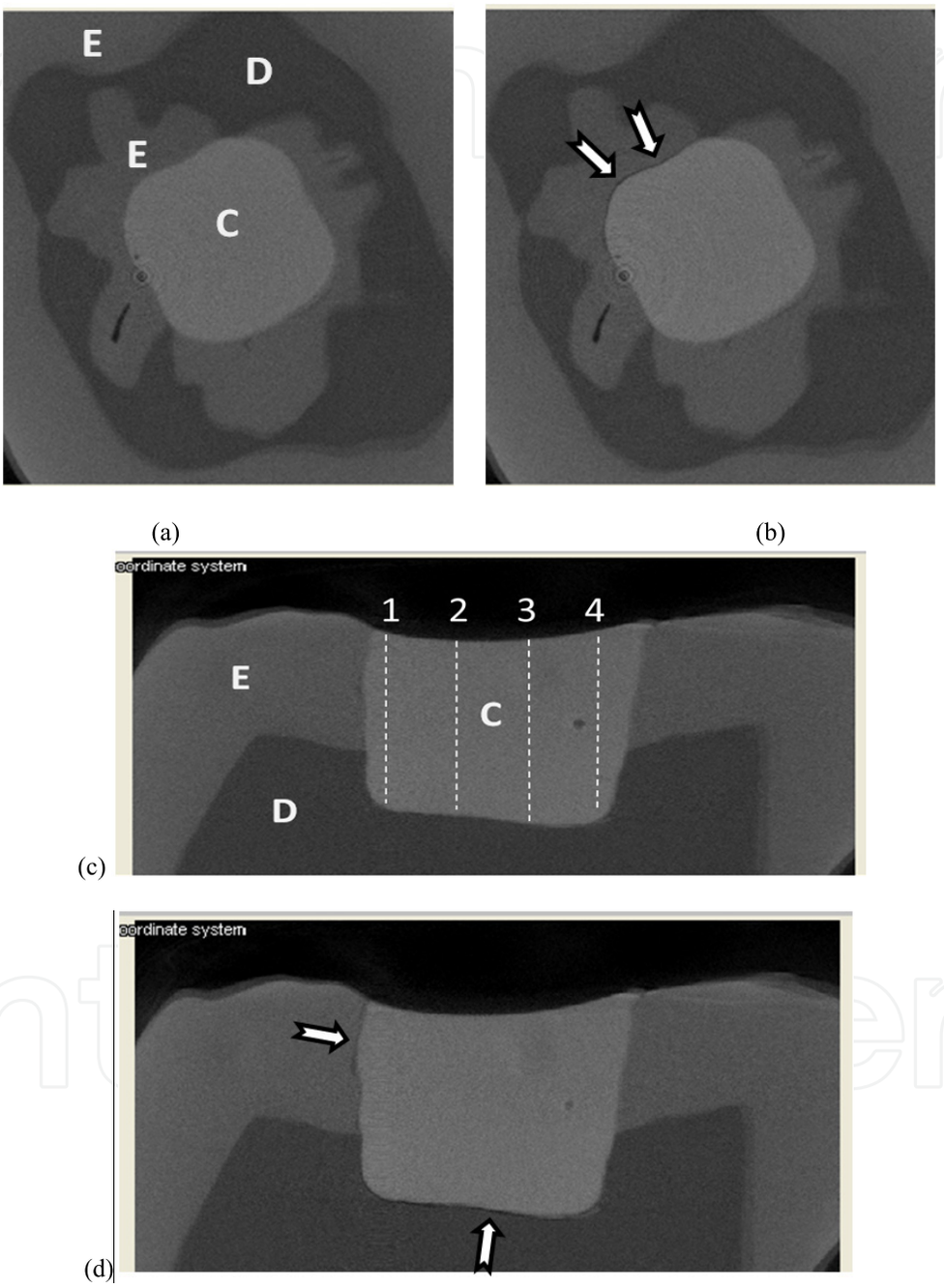

Figure 1. Micro-CT images of a tooth specimen restored with Z100: (a) horizontal cross-section before curing, (b) horizontal cross-section after curing, (c) vertical cross-section before curing and (d) vertical cross-section after curing. *(E-enamal, D-Dentin, C-composite. Lines 1-4 in (c) schematically indicate the locations of micro-hardness measurement described in Section 3.2.5 and Section 4.1. The arrows in (b) and (d) point out the debonding positions at the interface.)*

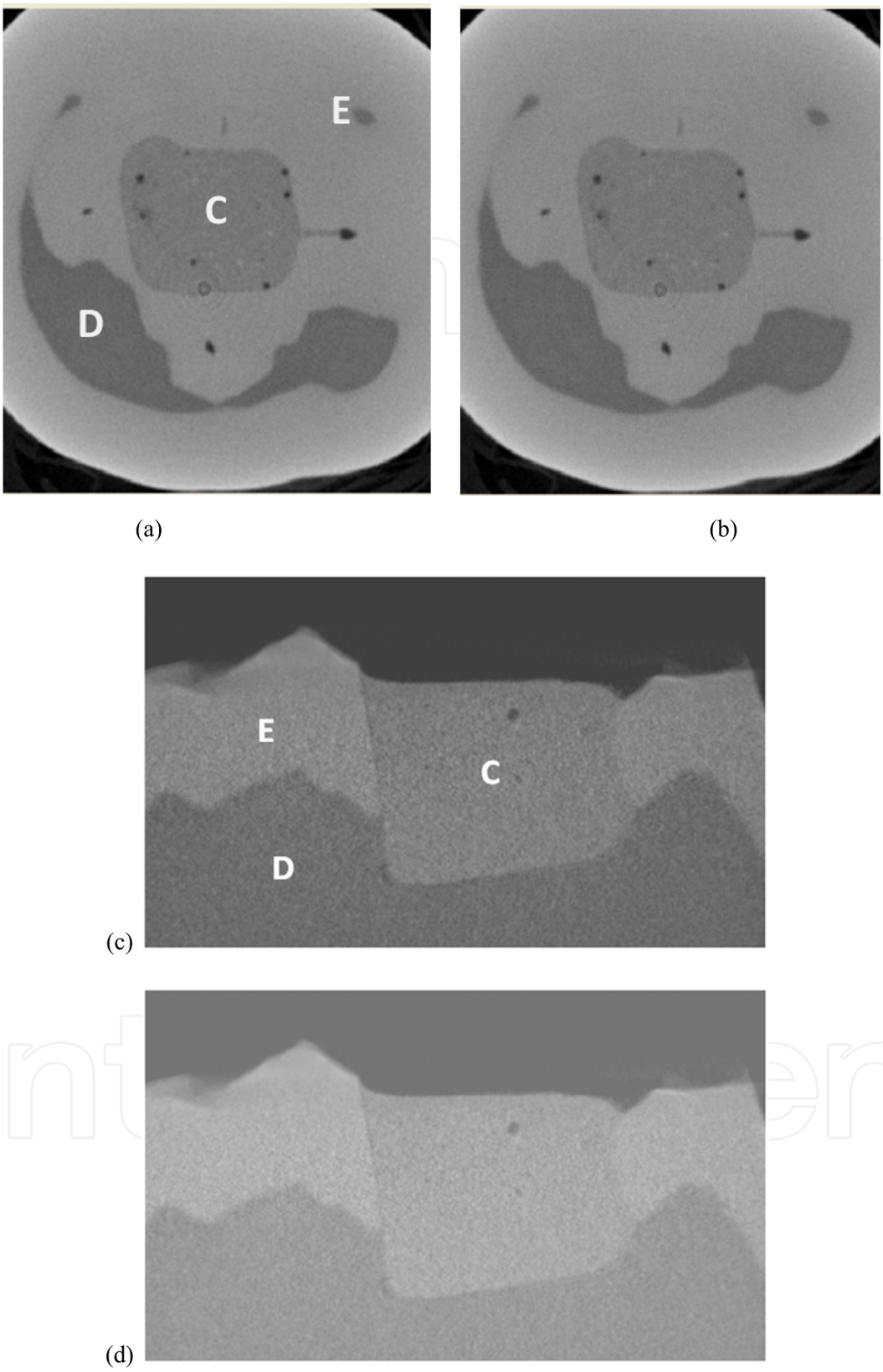

Figure 2. Micro-CT images of a tooth specimen restored with P90: (a) horizontal cross-section before curing, (b) horizontal cross-section after curing, (c) vertical cross-section before curing and (d) vertical cross-section after curing. *(Note: E-enamal, D-Dentin, C-composite.)*

Further details on the development of shrinkage stress in composite restorations and some current methods for assessing the resulting interfacial debonding are described in Section 2. The aim of this study is to develop a new method to evaluate the interfacial debonding of dental composite restorations. A non-destructive method, the acoustic emission (AE) technique, will be used to monitor *in-situ* the interfacial debonding of composite restorations during polymerization. The AE technique and the system used for monitoring interfacial debonding will be described in Section 3, where the capability of this new evaluation method will be verified by different tests. Then, in Section 4, the AE technique will be used to study the influences of several factors, including the composite material, C-factor (ratio between bonded and unbonded surfaces) and filling technique, on the debonding behavior of composite restorations.

2. Shrinkage stress and interfacial debonding in dental composite restorations

The dental resin composite is a mixture of organic monomer systems and inorganic filler particles. The monomer systems, which act as a matrix for the dental composite, are flowable before curing so that the composite can be easily packed into the tooth cavity and achieve good marginal adaptation with the tooth tissues. When polymerization is activated, the resin matrix will solidify, with its mechanical properties (Young's modulus, viscosity, hardness, strength, etc.) changing significantly and rapidly in the process. Volumetric shrinkage also occurs during polymerization due to the reduction of intermolecular separations in the monomers [12]. This is a very quick process which normally takes place within the first 30-50 seconds. The volumetric contraction that accompanies polymerization is typically on the order of 1.5–5% [1].

For most dental composite restorations, a bonding agent (adhesive) is used to create a strong bond at the tooth-composite interface. Thus, during the polymerization process, because the composite is constrained along the interfaces, shrinkage stresses are built up within the composite and tooth structure. These shrinkage stresses are difficult to predict or measure because of the small but complicated tooth geometry and rapidly changing material properties. Some experimental methods using simple specimens have been developed to estimate the polymerization shrinkage stress that develops in dental composites [1, 13, 14]. However, the measured shrinkage stresses are sensitive to the test configuration and procedures, e.g. the instrument's compliance, direction of curing light application and specimen shape. Also, because the material parameters (shrinkage strain, viscosity, Young's modulus and Poisson's ratio) of the composite that control the development of shrinkage stresses all change rapidly with time during polymerization, even with a suitable mathematical model, the accurate prediction of the shrinkage stresses is not trivial [15, 16].

If the shrinkage stress within a composite restoration is high enough, interfacial debonding or, more generally, failure between the tooth and restoration will occur. Interfacial failure can be adhesive, in which case failure occurs right in the adhesive layer; or it can be cohesive, in which case failure occurs in the tooth or composite materials near the interface.

Interfacial debonding has been identified as one of the main causes for replacement of composite restorations [2-4].

To date, there is no reliable tool to detect or monitor debonding between the composite and tooth during the curing process. Traditional methods for studying the interfacial integrity of dental restorations include optical microscopy, scanning electron microscopy (SEM) and transmission electron microscopy (TEM) [5-8, 17, 18]. The major disadvantage of these methods is that they are limited to essentially surface examination; internal debonding cannot be detected. To see whether debonding has occurred inside the restoration, these methods require destructive sectioning of the specimens which may introduce more uncertainties to the results due to possible machining damage. As an alternative, non-destructive methods, such as X-ray micro-computed tomography (micro-CT), have received much attention in recent years in the study of interfacial bonding/debonding of composite restorations [19]. Micro-CT is a computer-aided, 3D reconstruction of a structure or material that can be sliced virtually along any direction to gain accurate information on their internal geometric properties and structural parameters. Figures 1 and 2 show Micro-CT images used to study the interfacial debonding of composite restorations. Although Micro-CT can provide 3D examinations of the whole structure, its lower resolution means that it cannot detect debonding at a submicron level. Most of all, none of these imaging techniques can be used to monitor debonding as it happens.

3. AE technique and its application to interfacial debonding examination

3.1. The acoustic emission (AE) measurement technique

The acoustic emission (AE) measurement technique is also a non-destructive method. It is normally used to monitor the integrity of structures by providing real-time information of the fracture or damage process. It uses transducers or sensors to detect the high-frequency sound waves produced as a result of the sudden strain energy released within a material following fracture. Figure 3 shows schematically how an AE test system works. First, the cracking event within a material is captured by the AE sensor attached on the surface of the component. The raw signal is then passed through a preamplifier for pre-amplification and then to the acquisition system for acquisition and storage. Finally, the AE data can be displayed and analyzed by specially designed software.

AE technology has been widely used in research and industry to monitor the development of crack growth, wear, fiber-matrix debonding in composites, phase transformation, etc [20-22]. It has also been used to detect the fracture of different dental structures. For example, Ereifej et al. [23] used the AE technique to detect the initial fracture of ceramic crowns; Vallittu [24] used it to study the fracture of a composite veneer reinforced by woven glass fibres; and Kim and Okuno [25] used it to study the micro-fracture behavior of composite resins containing irregular-shaped fillers.

The interfacial debonding in composite restorations, either adhesive or cohesive, is actually a kind of fracture within the restored tooth structure. Therefore, it is possible to use the AE

technique to capture the cracking events. Unlike some of the imaging methods mentioned above, the AE method does not need destructive sample preparation and is not affected by the curing light. Therefore, it can be used to measure interfacial debonding in real time during the curing process, which cannot be achieved by micro-CT despite it being a nondestructive method as well.

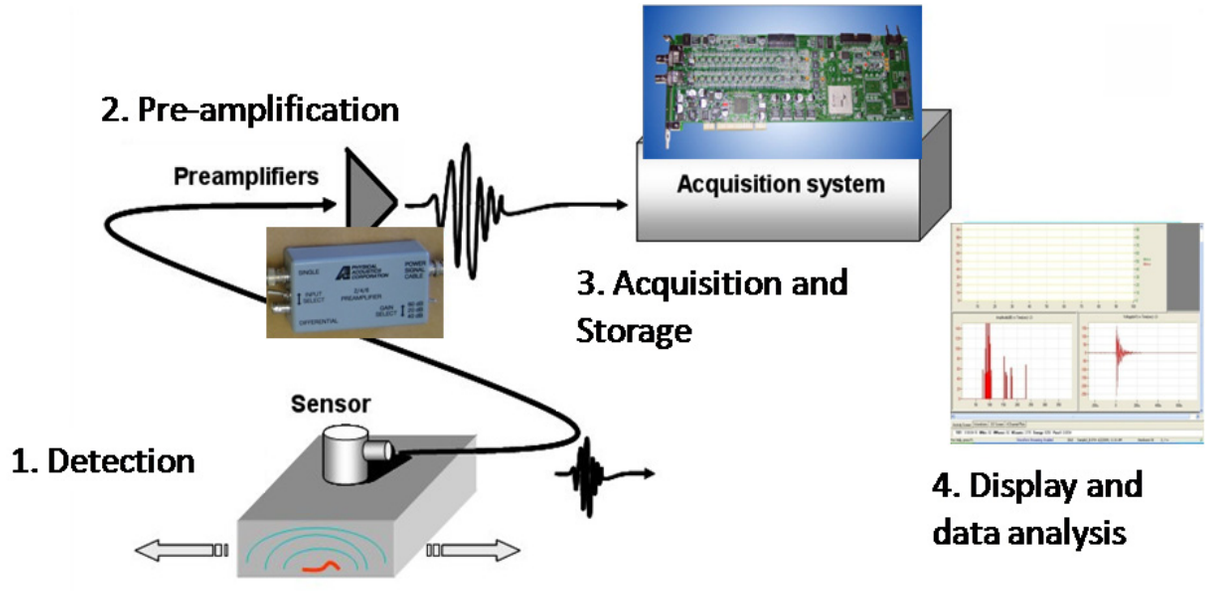

Figure 3. Schematic diagram of the AE test system

3.2. Application of AE technique to debonding measurement [26]

When using the AE technique to study interfacial debonding of dental restorations, it is necessary to prove that the captured AE signals indeed represent the cracking/micro-cracking events caused by interfacial debonding during curing of the composite. To this end, three groups of tests with different boundary constraints were designed and conducted, as described in this sub-section.

3.2.1. Specimens and materials

Figure 4 shows the specimens used in the three groups of tests: (a) free standing pea-size specimens of composite placed directly on the AE sensor, (b) ring specimens prepared from the root of a single bovine tooth and (c) intact human molars with a Class-I restoration. The composites in Group a were constrained least while those in Group c were constrained most. Each group had 4 specimens and Z100™ (3M ESPE) was the composite material used. More details of the specimens are given below.

The free-standing pea-size specimens of Group a were about 5mm in diameter. They were directly placed on the AE sensor without using any adhesive material, as shown in Figure 4(a). Each of these specimens was cured with a blue light (Elipar TriLight, 3M ESPE, US) at an intensity of 550mW/cm^2 for 40s. Testing with these specimens helped to verify that free shrinkage of the composite resin itself did not induce any AE event.

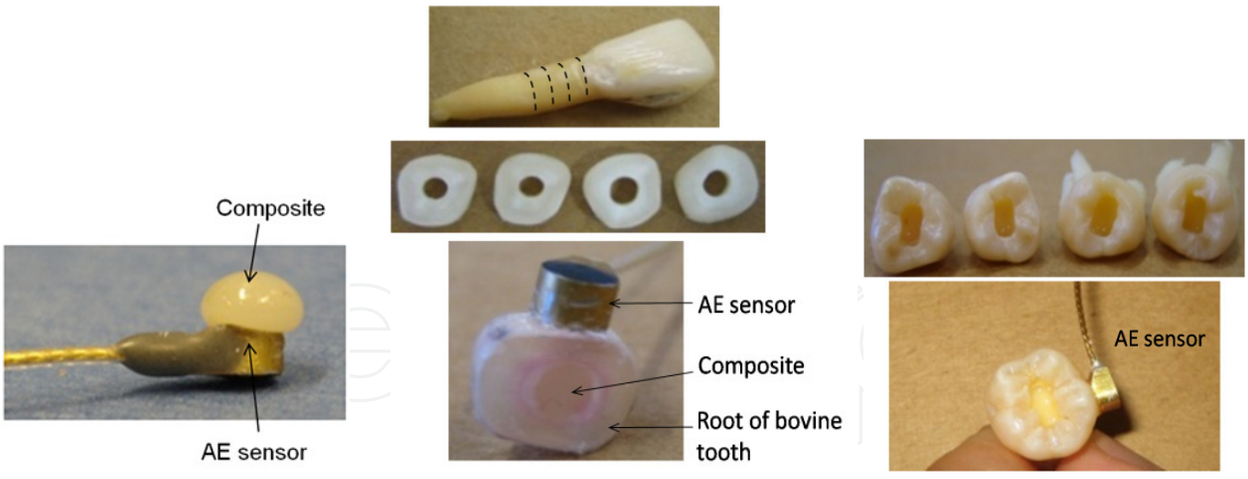

Figure 4. Samples: (a) pea-size composite specimen directly attached to the AE sensor, (b) rings prepared from the root of a bovine tooth and (c) human teeth with Class-I cavities

The four ring specimens in Group b were cut from the root of a single bovine tooth. They were, therefore, similar in material properties and structural anatomy; see Figure 4(b). The central holes of the specimens were originally the root canal, which was enlarged to 3mm in diameter with a high-speed handpiece. Compared with the whole tooth specimens in Group c, the composites in the ring specimens had larger free surface areas. This allowed the effect of the so-called C-factor (ratio between the bonded and unbonded surfaces) on interfacial debonding to be investigated.

For Group c, 4 intact human molars with similar dimensions were selected; they had been extracted and stored in saturated thymol solution at 4°C for less than one month. Standard Class-I cavities were prepared on these teeth by a single operator following clinical procedures with a high-speed handpiece and dental cutting burs; see Figure 4(c). The whole tooth specimens were considered to be the most representative of those in real clinical situations.

Each of the ring and tooth specimens was first treated with a bonding agent (Adper™ Scotchbond™ SE Self-Etch, 3M ESPE, US) to the cavity surface and then restored with the composite resin Z100™ (3M ESPE, US). Again, the composite was cured with a blue light (Elipar TriLight, 3M ESPE, US) at 550mW/cm² for 40s.

3.2.2. Shrinkage stress measurement

To explain the different levels of interfacial debonding measured by the AE method for different composite materials, the development of shrinkage stress for the composite materials during curing were measured using a tensometer (American Dental Association Foundation) [27]. This device is based on the basic engineering cantilever beam bending theory. The tensile force generated by the shrinking composite was calculated from the beam deflection using a previously obtained calibration constant. Further details of the

shrinkage stress measuring method using the tensometer are given in Ref. [27]. Before placing the composite material between the two glass-rod holders at the free end of the cantilever beam, the end surfaces of the glass rods were first polished with 600-grit sandpaper, silanized with a porcelain primer (Bisco Inc., Schaumburg, IL, USA), and then applied with a layer of adhesive (Scotchbond Multi-purpose, 3M, St. Paul, MN, USA). The dimensions of the composite specimens were 6mm in diameter and 2mm in height. The temporal developments of shrinkage stress for Z100™ (3M ESPE, US) and Filtek P90 (3M, St. Paul, MN, USA) are plotted in Figure 5. As can be seen, the shrinkage stresses developed rapidly and reached their maximum values within the first 50s, with Z100 producing a much higher shrinkage stress than Filtek P90.

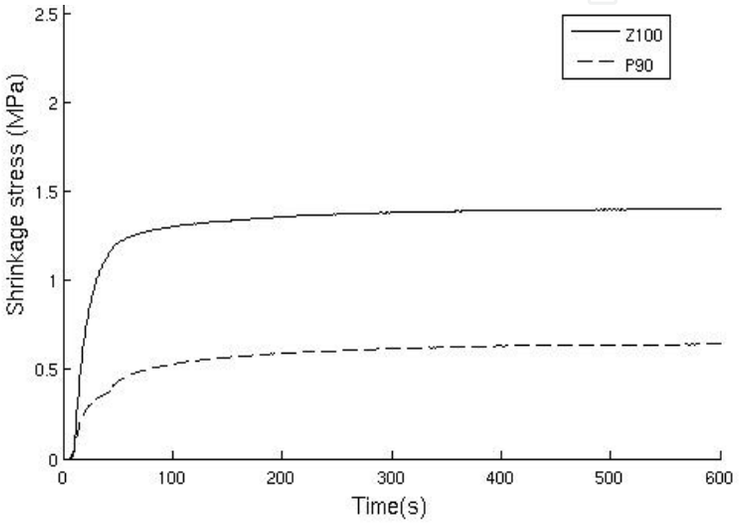

Figure 5. Shrinkage stress against time for Z100 and P90

3.2.3. AE measurement

A 2-channel AE system (PCI-2, Physical Acoustic Corporation, USA) was used in this study for AE data acquisition and digital signal processing. The AE sensor/transducer used for detecting interfacial debonding was S9225 (Physical Acoustic Corporation, USA), which had a resonance frequency of 250kHz. For the whole tooth and ring specimens, the AE sensor was attached to their outer surfaces using cyanoacrylate adhesive (Super Bond, Staples Inc, USA). The signals acquired with the sensor were amplified by a preamplifier with 20/40/60 dB gains. The parameters selected for the signal acquisition were: a 40dB gain for the preamplifier, a 100kHz-2MHz band pass and a 32dB threshold. These parameters were selected through many trial tests, with the aim of maximizing the system sensitivity while minimizing the background noises.

Figure 6 shows the procedures of a typical AE test on composite restoration debonding: (1) Prepare the cavity on a tooth sample; (2) Apply adhesive (bond agent) to cavity walls, fill the cavity with composite resin, and attach the AE sensor onto the tooth surface; (3) Turn on the AE system and blue curing light simultaneously. Cure the composite resin for 40s and record AE data continuously for 10 minutes. (4) Analyze the AE data. Use the curves of

instantaneous and accumulated AE events against time to study the curing behavior of the different specimens. During the AE tests, the teeth were wrapped by wet paper tissue to avoid cracking through dehydration.

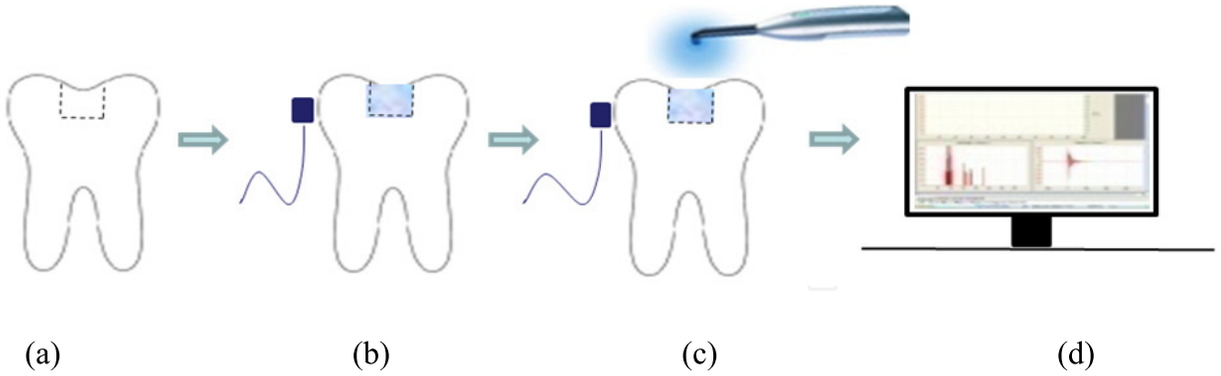

Figure 6. Procedure of an AE test on composite debonding: (a) sample preparation; (b) placement of adhesive, restoration, and AE sensor; (c) AE recording (10mins) & curing of composite resin (~40s); (d) AE data analysis

Figures 7 and 8 show the cumulative numbers of AE events against time for the ring specimens (Group b) and the human tooth specimens (Group c), respectively. The temporal development of the shrinkage stress of Z100, as shown in Figure 5, was also plotted for comparison. It was found that the temporal developments of the AE events followed roughly those of the shrinkage stress. It can also be seen that while some AE events occurred during the initial rapid polymerization of the composite resin, there were still some late events which took place a few minutes after the completion of light curing. In order to compare these two groups, the average temporal AE developments for Group b and Group c are plotted together in Figure 9, with the standard deviation of the cumulative number of AE events of each group being shown as red bars. No AE events were detected for the free-standing composite blob specimens (Group a) placed directly onto the AE sensor, illustrating that the free shrinkage of composite does not produce any AE event during curing. The mean and standard deviation of the total number of AE events for Group a, Group b and Group c were 0(-), 3.7(2.1) and 9.0(1.6), respectively, as summarized in Table 1.

3.2.4. Debonding evaluation using Micro-CT

The integrity of the tooth-restoration interface within the real tooth specimens (Group c) was examined further using a micro-CT machine (XT H 225, X-TEK Systems LTD). Two specimens were selected and they were first scanned immediately after placement of the composites to see how well they had adapted to the cavity walls. After curing and AE measurement, they were scanned for the second time to look for any detachment of the restoration from the cavity walls. In order to ensure the same position and orientation for the two scans to facilitate "same-slice" comparison, each of the specimens was mounted into a Teflon ring with positioning pins using an orthodontic resin (DENTSPLY International Inc., US). During scanning, the teeth were covered by wet paper tissue to avoid cracking through dehydration.

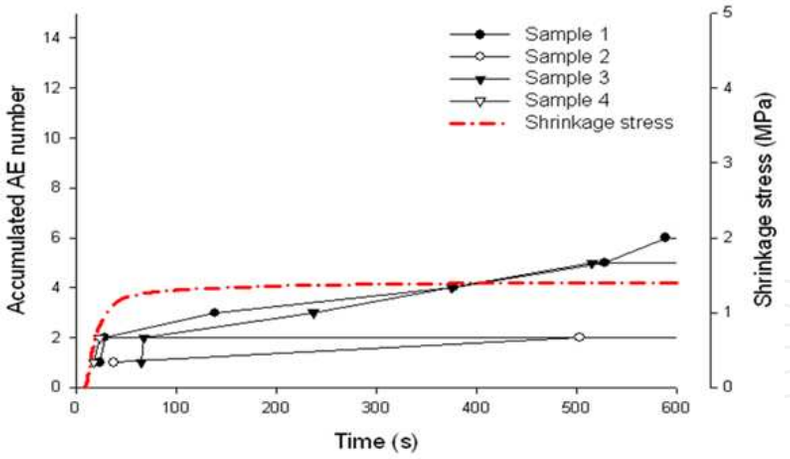

Figure 7. AE results for the ring specimens (Group-b)

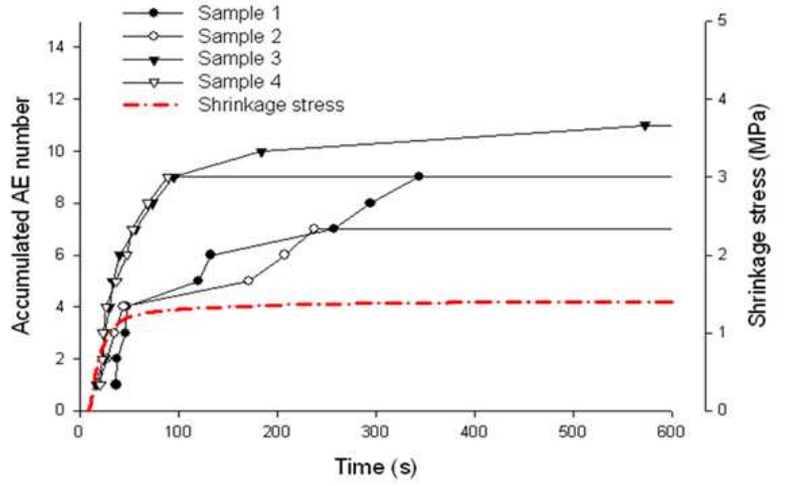

Figure 8. AE results for the real tooth specimens (Group-c)

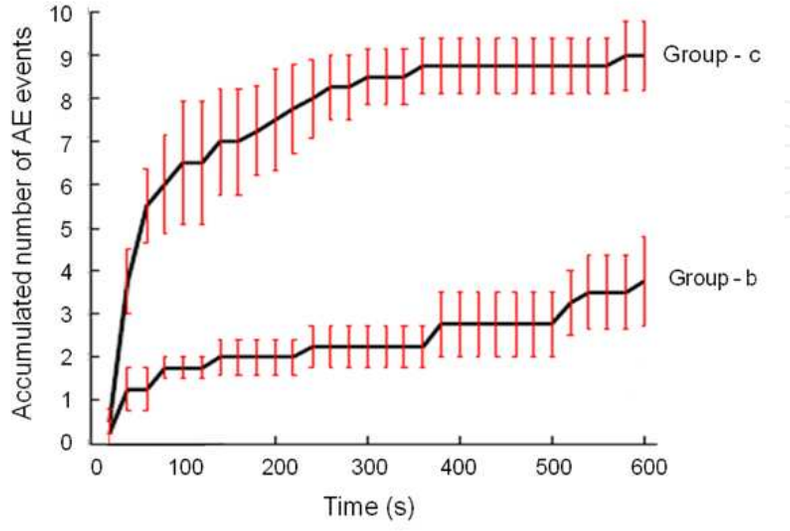

Figure 9. Average cumulative number of AE events for specimens in Groups b and c, with the standard deviation being plotted with red bars

	Group a	Group b	Group c
Mean	0	3.7	9.0
STD	-	2.1	1.6

Table 1. Total number of AE events: mean and standard deviation (STD)

The cross-sectional images obtained from the 3D Micro-CT reconstructions of one of the human tooth specimens restored with Z100 are shown in Figure 1. The micro-CT images clearly show the internal structures of the three main components of the restored teeth: enamel, dentin and composite. Before curing, as shown in Figures 1a and 1c, the composite can be seen to be perfectly in contact with the surrounding tooth tissues. After curing, however, the specimen showed clear interfacial debonding along the side walls and at the bottom of the cavity.

3.2.5. Micro-hardness measurement

To ensure that any lack of AE events/debonding was not due to uncured composite, the solidification of the composite within the tooth samples (Group c) after curing was assessed by using mico-hardness tests. After curing and AE measurement, one of the specimens was cut along a vertical central plane with a 102mm Dia. x 0.3mm thick diamond blade (Buehler, USA). The Vickers hardness was then measured with a micro-hardness testing machine (Micromet 5104, Buehler, USA). The indenter load was 100g and the load-holding time was 10s. The measurement points were located along 4 vertical lines within the restoration, which were schematically shown in Figure 1c. The measurement began from the top surface and continued until the bottom interface was reached.

Figure 10 shows the Vickers hardness of the cured composite (Z100) along its depth. It shows very uniform hardness distributions within the composite restoration, indicating that the polymerization of the composite resin was uniform and complete.

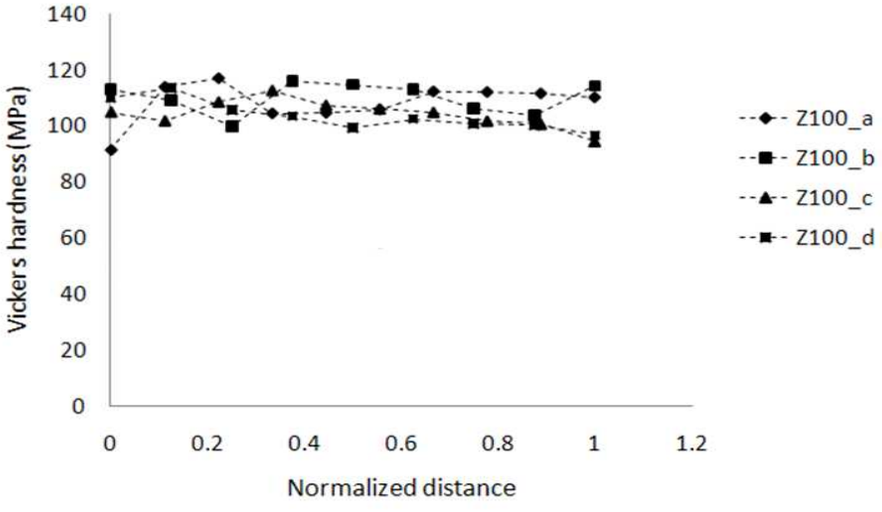

Figure 10. Vickers hardness along the depth of a Z100 restoration (see Figure 1c)

3.2.6. Discussion on the AE verification tests

From the AE results shown in Figures 7 and 8, it can be seen that the temporal developments of the AE events followed roughly those of the shrinkage stress. Also, polymerisation of the composite itself did not create any detectable AE events, as demonstrated by the negative results of the freestanding pea-size specimens placed directly on the sensor. All these indicate strongly that the cracking leading to the AE events in the restored samples were caused by the shrinkage stress produced by the polymerization of the composite resin.

Possible sources of AE events include debonding at the tooth-restoration interface and cohesive cracking in the tooth tissues or composite resin under the action of tensile shrinkage stresses. The only tensile stress in the ring specimens was the radial stress, which was maximum at the tooth-restoration interface. Therefore, cracking, either cohesive or adhesive, at the interface was the most possible reason causing those AE events in the ring specimens. The stress distributions within the restored tooth specimens were more complicated, due to the complex geometry involved. During shrinkage of the composite restoration, tensile stresses could also be induced in the axial direction, which would be maximum on the outer tooth surfaces. However, the micro-CT images of the tooth specimen, shown in Figure 1, confirm again that the AE events recorded were probably induced by adhesive debonding or cohesive cracking at the tooth-restoration interface.

Figure 9 shows that there were more AE events in the whole tooth specimens than there were in the ring specimens. This could be attributed to the larger restoration volume, and thus larger volumetric shrinkage, and/or the higher ratio of bonded-to-nonbonded surface area in the whole tooth specimens, i.e. the so-called C-factor. Also, the compliances of the two samples were different, with the ring specimens having a lower stiffness and thus a lower shrinkage stress, which led to fewer AE events. The more complicated geometry of the Class-I restorations also meant that local stress concentrations were more likely to exist in the tooth specimens which would lead to more debonding or AE events.

These results verified that the non-destructive AE measurement technique is an effective tool to detect and monitor *in-situ* the interfacial debonding of composite restorations during curing. It will allow quantitative studies to be carried out of the effects of factors such as composite material properties, cavity geometries, and restorative techniques on the integrity of the tooth-restoration interface.

4. Factors that affect interfacial debonding

There are many factors that can affect the initial quality and subsequent degradation of bonding at the tooth-restoration interface, e.g. properties of the composite and adhesive materials, cavity geometry, layering techniques, thermal and mechanical loading, etc. [5-8]. In this section, the influences of three factors on interfacial debonding will be studied using the AE technique described above. The three factors studied include: the composite material, the cavity configuration, and the filling technique.

4.1. Influence of the composite material

The interfacial debonding in composite restorations is mainly caused by the shrinkage stress produced during the polymerization of the composite. The material properties of the composite, i.e. the volume shrinkage, Young's modulus and strength, etc., will affect the internal shrinkage stress level and, thus, the degree of interfacial debonding. To investigate the influence of the composite resin on interfacial debonding, two commercial composite materials: Z100™ (3M ESPE, US) and Filtek™ P90 (3M ESPE, US) were chosen to conduct further AE debonding tests. The shrinkage stress curves for the two materials obtained using a tensometer (see Session 3.2.2) are shown in Figure 5. It can be seen that P90 produces a much lower shrinkage stress than Z100. This is because P90 is a low-shrinkage composite with special molecular structures that can open up to counter the shrinkage during polymerization.

8 intact human molars with similar dimensions were selected and randomly divided into 2 groups of 4. The specimen preparation and testing procedure and test equipments are the same as that in Section 3.2. The bonding agent used for all the specimens was Adper™ Scotchbond™ SE Self-Etch (3M ESPE, US).

Figure 11 shows the average temporal development of AE events during curing for the two groups, with the standard deviation being plotted with red bars. Just as it produced a lower shrinkage stress, Filtek P90 also produced a lower number of AE events than Z100, indicating that there was less interfacial debonding/cracking in the P90 specimens. In fact, two of the P90 specimens did not produce any detectable AE events at all.

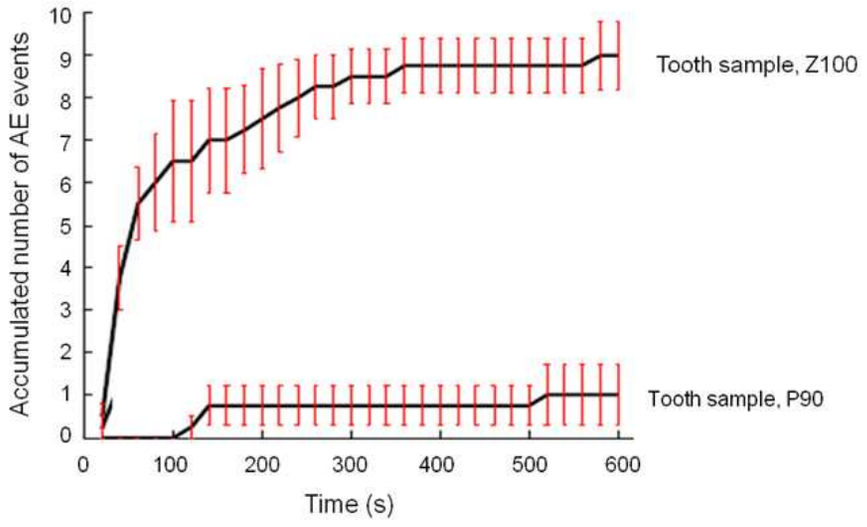

Figure 11. Average cumulative number of AE events for specimens restored with Z100 and P90 (the red bars show the standard deviation)

The above conclusion is supported by comparing the micro-CT images of the two specimens, as shown in Figures 1 and 2. After curing, the specimen restored with Z100 can be seen to have clear interfacial debonding along the walls and at the bottom of the cavity (Figures 1b and 1d), while that restored with P90 did not show any obvious debonding (Figures 2b and 2d).

Again, to discard the possibility that the low number of AE events in the P90 specimens was caused by incomplete polymerization, mico-hardness tests were also done on one of the specimens to assess the solidification of the composites. Figure 12 shows the Vickers hardness along the depth of the restoration for both Z100 and P90 specimens. It can be seen that, while Z100 was harder than P90, restorations of both materials had very uniform hardness distributions within them, indicating that the polymerization of all specimens were uniform and complete.

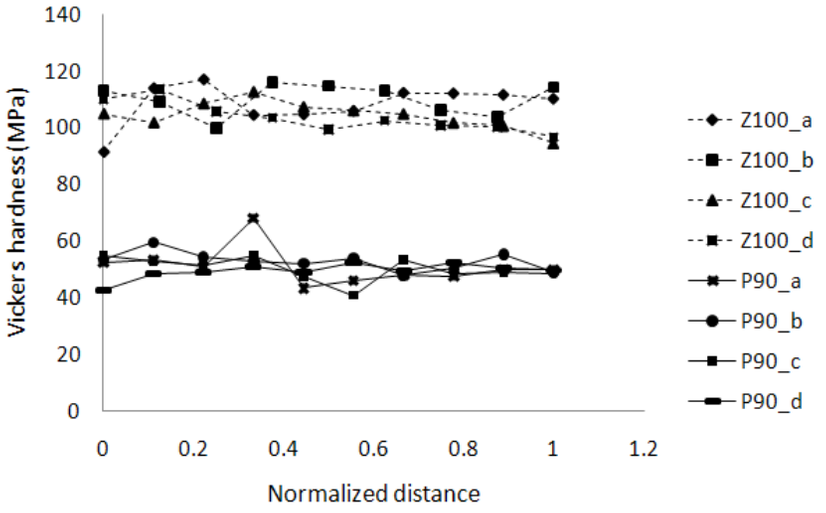

Figure 12. Vickers hardness along the depth of restoration (see Figure 1c) for specimens restored with P90. The results of Z100 specimens were plotted for comparison.

4.2. Influence of cavity configuration (C- factor) [28]

The C-factor of a restoration is defined as the ratio of the bonded areas to the unbonded areas, and it is normally used to characterize the configuration of the cavity [29]. Experimental studies [30-32] have shown that increasing the C-factor would reduce the interfacial bond strength and increase the incidence of interfacial failure. That was attributed to the higher shrinkage stress in restorations with a higher C-factor which had caused more interfacial debonding. In this section, three cavity configurations with different C-factors were used and their interfacial debonding was evaluated with the AE technique.

20 intact human molars with similar dimensions were selected and randomly divided into 4 groups of 5: Group 1 with large Class-I cavities, Group 2 with small Class-I cavities, Group 3 with small Class-II cavities and Group 4 with large Class-II cavities. The specimen preparation, testing procedure and test equipments were similar to those in Section 3.2 and Section 4.1. The bonding agent used for all the specimens was total-etch adhesive Adper™ Single Bond Plus (3M ESPE, USA) and the composite resin was Z100™ (3M ESPE, US). Figure 13 shows schematically the Class-I and Class-II cavities prepared and the dimensions of interest. The dimensions of each specimen were measured with a micrometer (Mitutoyo, Japan) with which the C-factor was calculated. The average C-factors of the four groups were 3.37, 2.90, 2.00 and 1.79, respectively, as summarized in Table 2.

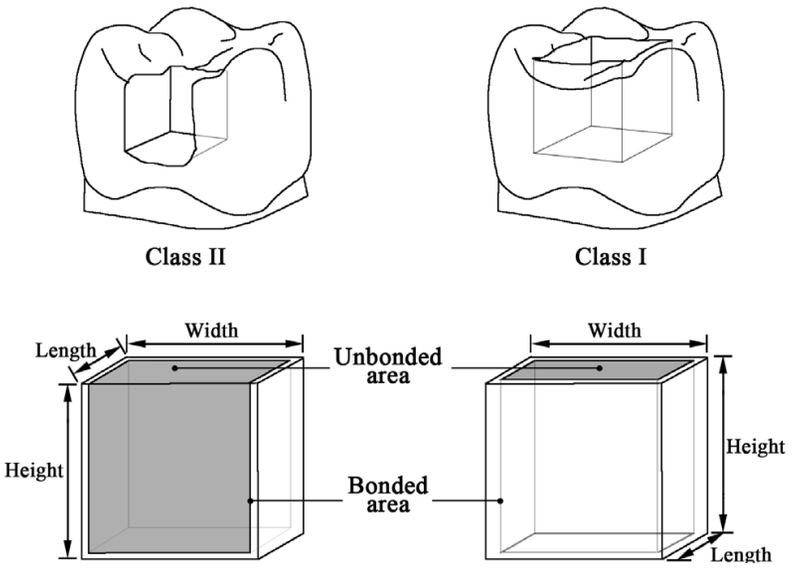

Figure 13. Schematic diagrams of the prepared tooth cavities with dimensions of interest. The shaded areas are the free, unbonded surface areas

Cavity type	Group	Length (mm)	Width (mm)	Depth (mm)	C-factor	Bond area (mm^2)	Volume (mm^3)
Class I	1	3.94	2.99	2.08	3.45	40.62	24.50
		3.76	3.68	1.88	3.02	41.81	26.01
		4.13	4.06	2.48	3.42	57.39	41.58
		4.00	3.79	2.02	3.08	46.63	30.62
		3.99	3.61	2.72	3.87	55.75	39.18
Mean (STD)		3.96(0.13)	3.63(0.39)	2.24(0.35)	3.37(0.34)	48.44(7.78)	30.68(7.72)
Class I	2	2.66	2.77	1.40	3.06	22.57	10.32
		3.29	3.04	1.80	3.28	32.79	18.00
		2.86	2.87	1.05	2.47	20.24	8.62
		3.59	2.70	1.10	2.43	23.53	10.66
		2.73	2.70	1.45	3.14	23.12	10.69
Mean (STD)		3.03(0.40)	2.82(0.14)	1.36(0.30)	2.88(0.40)	24.45(4.83)	11.66(3.65)
Class II	3	2.09	1.85	1.68	2.01	14.00	6.50
		2.35	1.92	1.42	1.92	13.91	6.41
		2.30	1.91	1.73	2.03	15.66	7.60
		2.39	1.94	2.02	2.13	18.21	9.37
		2.11	2.10	1.70	1.90	15.18	7.53
Mean (STD)		2.25(0.14)	1.94(0.09)	1.71(0.21)	2.00(0.09)	15.39(1.75)	7.48(1.19)
Class II	4	3.75	3.34	2.47	1.89	39.30	30.94
		4.18	3.39	2.72	1.97	46.13	38.54
		4.49	3.36	2.19	1.88	42.11	33.04
		3.63	3.51	1.58	1.63	29.76	20.13
		4.57	4.50	1.80	1.57	45.12	37.02
Mean (STD)		4.12(0.42)	3.62(0.50)	2.15(0.47)	1.79(0.18)	40.48(6.57)	31.93(7.26)

Table 2. Dimensions and geometrical factors of the specimens used in the experimental study on C-factor

Figure 14 shows the mean cumulative number of AE events against time for the four test groups, with the standard deviations shown as red bars. AE caused by interfacial debonding was first detected about 20s into the curing of the composite and developed rapidly thereafter. The mean and standard deviation of the total number of AE events for the four groups were 29.6±15.7, 10.0±5.8, 2.6±1.5, and 2.2±1.3 (Table 3), respectively, which showed an increase with an increasing C-factor. Table 4 shows the statistical significance (*p*-value) of the differences in the total number of AE events between the different groups. It can be seen that the differences were significant, except that between Groups 3 and 4 which had very similar C-factors.

In Figure 15(a), the total number of AE events for all the specimens were plotted against their individual C-factors. To account for the differences in the bonded area or volume of restorations with similar C-factors, the total number of AE events per unit bonded area and that per unit composite volume are plotted in Figure 15(b) and 15(c), respectively, for comparison. The mean and standard deviation of these normalized numbers for the 4 groups are also listed in Table 3. Despite the large variations in the number of AE events detected among specimens with similar C-factors, it can be clearly seen that the amount of debonding increased with an increase in the C-factor. There appeared to be a critical value for the C-factor associated with Z-100, i.e. 1.5, below which no AE events could be detected. The trend remained the same even when possible influence from the bonded area and restoration volume was taken into account.

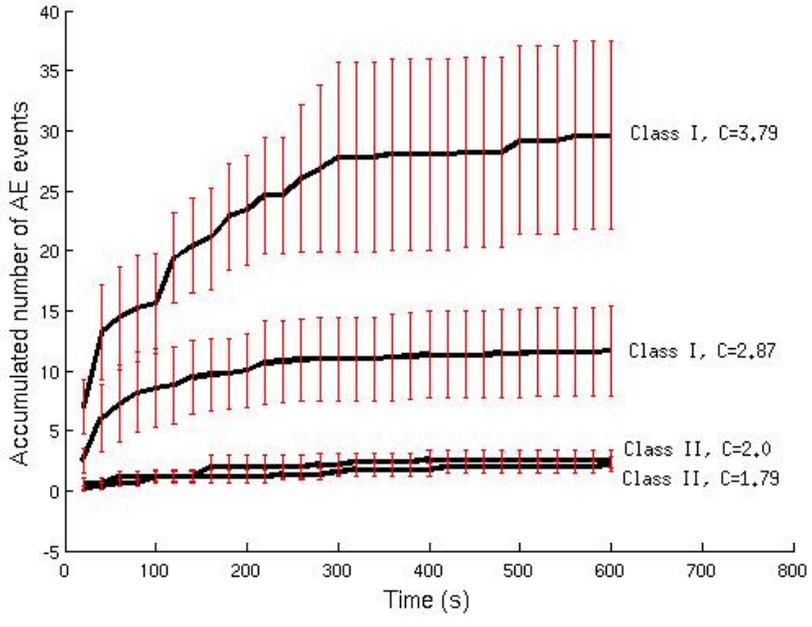

Figure 14. The cumulative number of AE events against time for the 4 test groups

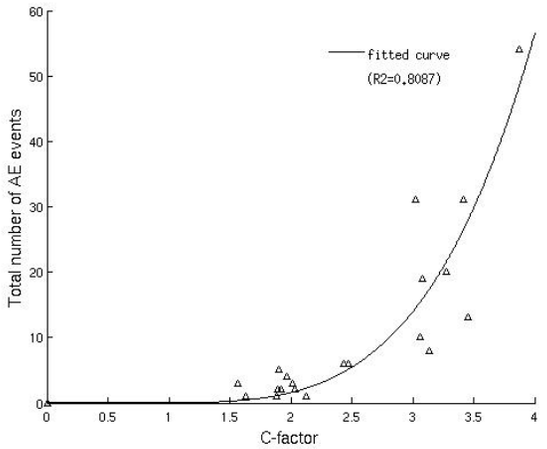

(a)

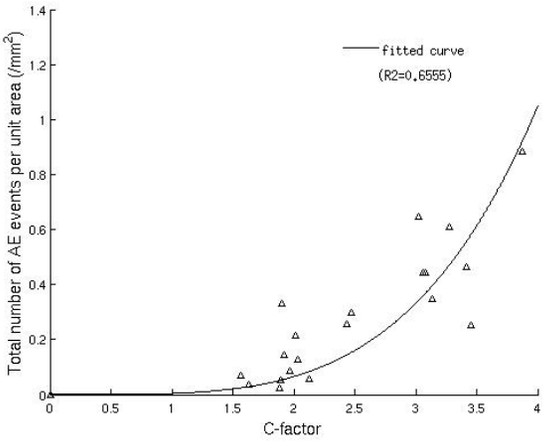

(b)

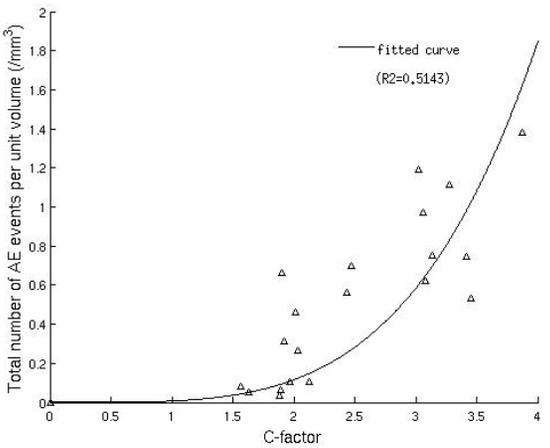

(c)

Figure 15. The total number of AE events as a function of the C-factor: (a) total number, (b) total number per unit bond area (/mm^2), and (c) total number per unit composite volume (/mm^3)

Group	Total number of AE events	Total number of AE events per area (/mm^2)	Total number of AE events per volume (/mm^3)
1	29.6 (15.7)	0.54(0.24)	0.89(0.37)
2	10.0 (5.8)	0.39(0.14)	0.81(0.22)
3	2.6 (1.5)	0.17(0.10)	0.36(0.21)
4	2.2 (1.3)	0.05(0.02)	0.07(0.03)

Table 3. Results from the AE tests: mean (standard deviation)

Group	2	3	4
1	0.031	0.005	0.005
2		0.025	0.019
3			0.667

Table 4. Statistical significance (*p*-value) of the difference in the total number of AE events between the groups with different C-factors

4.3. Influence of the filling technique

The composite placement techniques (bulk vs. incremental) have been shown to affect the magnitude of the polymerization shrinkage stresses and cuspal deformations in restored teeth [33-37]. Compared with the bulk filling method, the incremental filling method has been reported to produce lower shrinkage stresses. Therefore, the incremental filling method is expected to produce less interfacial debonding than the bulk filling method. This hypothesis will be tested in this section with the AE technique.

12 incisor bovine teeth with similar geometries were selected and randomly divided into 2 groups of 6. A cylindrical cavity, which was 2mm in depth and 4mm in diameter, was cut into the top surface of each tooth; see Figure 16(a). All samples were prepared by a single operator following typical clinical procedures with a high-speed handpiece and dental cutting burs. Each specimen was then treated with the bonding agent Adper™ Single Bond Plus (3M ESPE, USA) to the cavity surfaces and then restored with the composite resin Z100™ (3M ESPE, US) using either the bulk or incremental filling technique, as shown in Figure 16(b). The AE sensor was attached onto the opposite surface of the tooth. For the group restored with the incremental technique, recording of the AE events was interrupted in between placements of the 2 layers.

Figure 17 shows the total number of AE events for all the specimens. Note that 4 out of 6 of the specimens with the incremental filling method did not produce any AE events at all, while the remaining 2 produced only a small number of AE events. Compared with the incremental-filling group, specimens restored with the bulk-fill method produced much more AE events, indicating more interfacial debonding in those specimens.

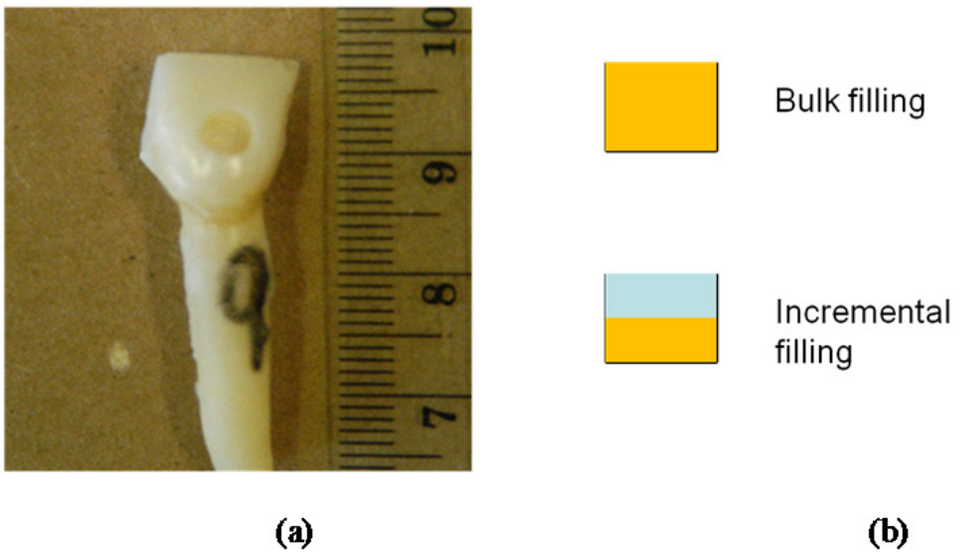

Figure 16. (a) Cylindrical cavity on a bovine tooth, and (b) the two different filling techniques

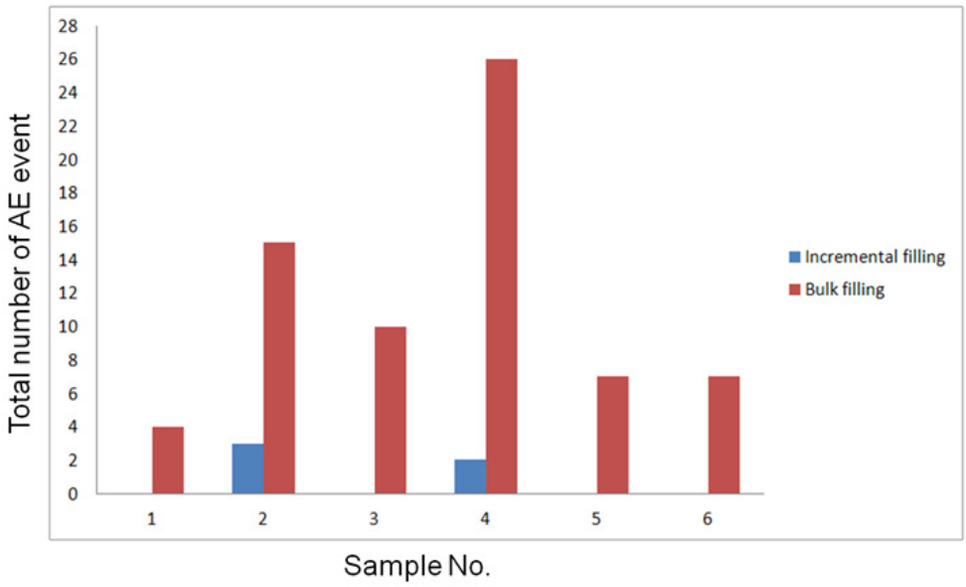

Figure 17. The total number of AE events for specimens restored with the bulk and incremental techniques

5. Discussion and concluding remarks

The AE technique, which is widely used for fracture monitoring in many areas, was for the first time introduced here to monitor *in-situ* the interfacial deboning of composite restorations. Its effectiveness was verified by several groups of experiments using specimens with different boundary constraints: freestanding blobs of composite, ring specimens cut from a tooth root and whole human molars. It was also shown from the AE results that interfacial debonding in composite restorations is greatly influenced by the restorative composite material, cavity configuration and filling technique. In general, composites with

lower shrinkage, cavities with smaller C-factors and use of the incremental filling method can produce less interfacial debonding. These findings agreed with the results from other researchers using different evaluative methods.

The AE technique has several advantages over the other methods in evaluating the interfacial debonding of dental composite restorations: 1) it is non-destructive; 2) it is not affected by the light-curing process and can therefore be used to make *in-situ* measurement during the curing; and 3) it is very sensitive, being able to detect micro-cracking that cannot be seen by micro-CT. However, there are still certain limitations to the AE technique. The AE results are dependent on the operational parameters of the AE system, e.g. the signal threshold, band pass, and the gain of the preamplifier. Therefore, it is important to specify those parameters when comparing AE results from different AE measurements. Also, false signals which have similar frequencies with the interfacial debonding may not be filtered out. Efforts are therefore needed to minimize such false signals, e.g. by keeping the tooth samples wet to avoid enamel cracking caused by dehydration. Finally, unlike the optical methods, the AE technique cannot provide direct visual images of the interfacial debonding.

In the future, more efforts should be made to increase the amount of information the AE technique can provide in evaluating interfacial debonding in dental composite restorations. For example, it may be possible to locate the source of the AE events by using the times-of-arrival captured by several AE sensors placed at different positions on the tooth [38-40]. This will help to establish where the critical regions of debonding are in a restored tooth. Also, the AE technique can be used to study other factors that may influence interfacial debonding, e.g. the adhesive/bonding agent, cavity shapes (with a constant C-factor), environmental challenges such as thermal and occlusal load, etc. Overall, it is a powerful tool which can be used to evaluate the interfacial debonding of composite restorations under more clinically relevant conditions in a more systematic way. This will help to improve the quality of bonding at the tooth-restoration interface and, thus, increase the longevity of composite restorations.

Author details

Haiyan Li, Jianying Li and Alex Fok
Minnesota Dental Research Center for Biomaterials and Biomechanics, School of Dentistry, University of Minnesota, Minneapolis, MN, United States

Xiaozhou Liu
China Medical University School and Hospital of Stomatology, Shenyang, PR China

Acknowledgement

The authors would like to acknowledge 3M ESPE for providing the restorative materials and the Minnesota Dental Research Center for Biomaterials and Biomechanics (MDRCBB) for providing the test devices. They also acknowledge Mr. Xiaofei Yun and Mr. Max Hofer

for their contributions to the AE tests. Xiaozhou Liu would like to thank the China Scholarship Council and the MDRCBB for financially supporting her study visit to the MDRCBB.

6. References

[1] Ferracane, J.L., *Developing a more complete understanding of stresses produced in dental composites during polymerization*. Dental Materials 2005. 11: p. 7.
[2] Forss, H. and E. Widstrom, *Reasons for restorative therapy and the longevity of restorations in adults*. Acta Odontol Scand 2004. 62: p. 5.
[3] Dauvillier, B.S., M.P. Aarnts, and A.J. Feilzer, *Developments in shrinkage control of adhesive restoratives.* Jounal of Esthetic Dentistry, 2000. 12: p. 9.
[4] Brunthaler, A., et al., *Longevity of direct resin composite restorations in posterior teeth.* Clinical Oral Investigations 2003. 7: p. 8.
[5] Yap, A.U.J., et al., *An in vitro microleakage study of three restorative techniques for class II restorations in posterior teeth*. Biomaterials, 1996. 17: p. 5.
[6] Lopes, G.C., M. Franke, and H.P. Maia, *Effect of finishing time and techniques on marginal sealing ability of two composite restorative materials*. Journal of Prosthetic Dentistry 2002. 88: p. 5.
[7] Abdalla, A.I. and C.L. Davidson, *Effect of mechanical load cycling on the marginal integrity of adhesive class I resin composite restorations*. Journal of Dentistry 1996. 24: p. 4.
[8] Ausiello, P., et al., *Debonding of adhesively restored deep class II MOD restorations after functional loading*. American Journal of Dentistry, 1999. 12: p. 5.
[9] Shono, Y., et al., *Effects of cross-sectional area on resin-enamel tensile bond strength*. Dental Materials, 1997. 13: p. 7.
[10] Goracci, C., et al., *Influence of substrate, shape, and thickness on microtensile specimens' structural integrity and their measured bond strengths*. Dental Materials 2004. 20: p. 12.
[11] Phrukkanon, S., M.F. Burrow, and M.J. Tyas, *The influence of crosssectional shape and surface area on the microtensile bond test*. Dental Materials 1998. 14: p. 10.
[12] McMurray, J., *Fundamentals of Organic Chemistry*1986, Monterey, CA: Brooks/Cole.
[13] Watts, D.C., A.S. Marouf, and A.M. Al-Hindi, *Photo-polymerization shrinkage-stress kinetics in resin-composites: methods development*. Dental materials 2003. 19: p. 11.
[14] Gonçalves, F., et al., *Contraction Stress Determinants in Dimethacrylate Composites.* Journal of Dental Reseach, 2008. 87: p. 5.
[15] Li, J., *The Biomaterials And Biomechanics Of Dental Restorations: Property Measurement And Simulation*, 2008, University of Manchester.
[16] Li, J., H. Li, and S.L. Fok, *A mathematical analysis of shrinkage stress development in dental composite restorations during resin polymerization*. Dental materials 2008. 24: p. 9.
[17] Kanemura, N., H. Sano, and J. Tagami, *Tensile bond strength to and SEM evaluation of ground and intact enamel surfaces*. Journal of Dentistry, 1999. 27: p. 8.
[18] Sano, H., et al., *Comparative SEM and TEM observations of nanoleakage within the hybrid layer*. Operative Dentistry 1995. 20: p. 8.
[19] Santis, R.D., et al., *A 3D analysis of mechanically stressed dentin–adhesive–composite interfaces using X-ray micro-CT*. Biomaterials, 2005. 26: p. 14.
[20] Nair, A. and C.S. Cai, *Acoustic emission monitoring of bridges: Review and case studies.* Engineering Structures, 2010. 32(6): p. 1704-1714.

[21] Bohse, J., *Acoustic emission characteristics of micro-failure processes in polymer blends and composites*. Composites Science and Technology, 2000. 60(8): p. 1213-1226.
[22] Skåre, T. and F. Krantz, *Wear and frictional behaviour of high strength steel in stamping monitored by acoustic emission technique*. Wear, 2003. 255(7–12): p. 1471-1479.
[23] Ereifej, N., N. Silikas, and D.C. Watts, *Initial versus final fracture of metal-free crowns, analyzed via acoustic emission.* Dental Materials, 2008. 24(9): p. 1289-1295.
[24] Vallittu, P.K., *Use of woven glass fibres to reinforce a composite veneer. A fracture resistance and acoustic emission study*. Journal of Oral Rehabilitation, 2002. 29: p. 7.
[25] Kim, K.H. and O. Okuno, *Microfracture behaviour of composite resins containing irregular-shaped fillers Journal of Oral Rehabilitation*, 2002. 29: p. 7.
[26] Li, H., et al., *Non-destructive examination of interfacial debonding using acoustic emission*. Dental Materials, 2011. 27: p. 8.
[27] Lu, H., et al., *Probing the origins and control of shrinkage stress in dental resin-composites: I. Shrinkage stress characterization technique*. Journal of Materials Science: Materials in Medicine, 2004. 15: p. 7.
[28] Liu, X., et al., *An acoustic emission study on interfacial debonding in composite restorations*. Dental Materials, 2011. 27: p. 8.
[29] Braga, R.R., et al., *Influence of cavity dimensions and their derivatives (volume and 'C' factor) on shrinkage stress development and microleakage of composite restorations*. Dental Materials, 2006. 22(9): p. 818-823.
[30] Feilzer, A.J., A.J.D. Gee, and C.L. Davidson, *Setting stress in composite resin in relation to configuration of the restoration*. J Dent Res, 1987. 66(11): p. 4.
[31] Nikolaenko, S.A., et al., *Influence of c-factor and layering technique on microtensile bond strength to dentin.* Dental Materials, 2004. 20(6): p. 579-585.
[32] Watts, D.C. and J.D. Satterthwaite, *Axial shrinkage-stress depends upon both C-factor and composite mass.* Dental Materials, 2008. 24(1): p. 1-8.
[33] Park, J., et al., *How should composite be layered to reduce shrinkage stress: Incremental or bulk filling*? Dental Materials, 2008. 24(11): p. 1501-1505.
[34] McCullock, A. and B. Smith, *In vitro studies of cuspal movement produced by adhesive restorative materials.* Br Dent J, 1986. 161: p. 5.
[35] Lee, M.-R., et al., *Influence of cavity dimension and restoration methods on the cusp deflection of premolars in composite restoration*. Dental Materials, 2007. 23(3): p. 288-295.
[36] Versluis, A. and W. Douglas, *Does an incremental filling technique reduce polymerization shrinkage stresses?* . J Dent Res, 1996. 75: p. 8.
[37] Abbas, G., et al., *Cuspal movement and microleakage in premolar teeth restored with a packable composite cured in bulk or in increments*. J Dent Res, 2003. 31: p. 8.
[38] Mavrogordato, M., et al., *Real time monitoring of progressive damage during loading of a simplified total hip stem construct using embedded acoustic emission sensors. Medical Engineering &* Physics, 2011. 33(4): p. 395-406.
[39] Lympertos, E.M. and E.S. Dermatas, *Acoustic emission source location in dispersive media.* Signal Processing, 2007. 87(12): p. 3218-3225.
[40] Salinas, V., et al., *Localization algorithm for acoustic emission.* Physics Procedia, 2010. 3(1): p. 863-871.